JOURNAL OF MATERIALS SCIENCE **34** (1999) 45–52

Characterization and optimization of the coercivity-modifying nitrogenation and re-calcination process for strontium hexaferrite powder synthesized conventionally

S. A. S. EBRAHIMI*, C. B. PONTON, I. R. HARRIS
School of Metallurgy and Materials, The University of Birmingham, Edgbaston, Birmingham, B15 2TT, UK

A. KIANVASH
Department of Ceramic Engineering, Faculty of Engineering, The University of Tabriz, Tabriz 51 664, Iran

Strontium hexaferrite powder synthesized conventionally in-house from strontium carbonate and hematite (Fe_2O_3) without using additives has been treated in a static nitrogen atmosphere and subsequently calcined in static air. The phase identification studies by means of X-ray diffraction (XRD) and thermal magnetic analysis (TMA) indicated the decomposition of the strontium hexaferrite and the reduction of the resultant iron oxide (Fe_2O_3) during the reaction with nitrogen. High-resolution scanning electron microscopy (HRSEM) studies show that the reduction occurring during nitrogenation results in the conversion of some of the large grains into much finer sub-grains. Strontium hexaferrite, Fe_3O_4, and $Sr_7Fe_{10}O_{22}$ were the main phases obtained after reduction. However, weak traces of other phases, such as Fe_2O_3, were also detected. The hexaferrite phase re-formed on subsequent calcination. The magnetic measurements indicated a significant decrease in the intrinsic coercivity during nitrogenation due to the formation of Fe_3O_4. However, after a re-calcination process, the remanence and maximum magnetization (i.e., magnetization at 1100 kA/m) exhibited values close to the initial values before treatment, but the value of the intrinsic coercivity was higher than that prior to nitrogenation. Examination of the re-calcined microstructure showed that this could be attributed to the fine grains that originated from the fine sub-grain structures formed in the powder particles during nitrogenation.

The optimum time, initial gas pressure, and temperature of nitrogenation and the optimum temperature of re-calcination were investigated using a vibrating sample magnetometer (VSM), XRD, and HRSEM. The optimum temperature for nitrogenation was 950 and 1000 °C for re-calcination. The optimum time and initial nitrogen pressure were 5 h and 1 bar, respectively. The highest intrinsic coercivity obtained after re-calcination was ~340 kA/m.

1. Introduction

A novel method of processing hexaferrites to produce an increased intrinsic coercivity has been patented and reported for commercial and hydrothermally synthesized materials [1, 2]. By this method, low coercivity can be produced by heat-treating the powders in the presence of hydrogen, nitrogen, or carbon. High coercivity can then be achieved by a post-gas treatment calcination in air. Subsequently, the effect of hydrogen and nitrogen on in-house conventionally synthesized strontium hexaferrite was investigated and higher values of intrinsic coercivity produced [3]. Following these earlier studies, additional work has been carried out to optimize the hydrogenation and re-calcination processes for conventionally synthesized strontium hexaferrite powder and hence its magnetic properties [4]. The phase transformations and changes in magnetic properties during the dynamic hydrogenation and subsequent re-calcination treatment will be reported elsewhere [5].

This paper describes the research conducted to likewise optimize the nitrogenation and re-calcination processes for conventionally synthesized strontium

* Also Department of Metallurgy, Faculty of Engineering, Tehran University, P.O. Box 11365-4563, Tehran, Iran.

hexaferrite powder to compare the optimized hydrogenation/re-calcination process with the optimized nitrogenation/re-calcination process in a subsequent paper [6]. The characterization techniques used in the present work were X-ray diffraction (XRD), thermomagnetic analysis (TMA), vibrating sample magnetometery (VSM), and high-resolution scanning electron microscopy (HRSEM). The phase transformations during the nitrogenation and recalcination processes are identified. The variations in the magnetic properties at each stage are described in relation to the phase composition and particle/grain morphology. Finally, the optimized time, temperature, and initial pressure for the nitrogenation process and the optimized re-calcination temperature have been determined.

This process provides a wide range of coercivities as a result of the different steps and step-combinations possible that could increase the use and range of applications.

2. Experimental procedure

The starting material was M-type strontium hexaferrite ($SrFe_{12}O_{19}$) produced in-house conventionally from strontium carbonate ($SrCO_3$) and iron oxide (α-Fe_2O_3) without additives. The details of the production of the hexaferrite powder have been described previously [4]. The nitrogenation was carried out in a static atmosphere employing various initial gas pressures. The amount of powder in each batch was 4 g. The nitrogenation process consisted of heating the powder at a rate of 5 °C/min to different temperatures in a resistance-heated vacuum tube furnace and dwelling for various times before cooling at the same rate.

The subsequent calcination process consisted of heating the powder in static air to different temperatures in a resistance-heated muffle furnace, dwelling for 1 h, and then cooling. The heating and cooling rates were 5 °C/min and 10 °C/min, respectively. The treated powder was subjected to a light milling process prior to the magnetic measurements. The magnetic properties were measured at room temperature using a VSM operating up to a maximum field of 1100 kA/m. The magnetization at this field is referred to as the maximum magnetization (M_m) in this work. The majority of VSM samples were set in molten wax but were not subjected to a magnetic alignment field and so were magnetically isotropic. On applying a field, there was no evidence of anisotropy in the treated powders. XRD (CoK_α radiation) was used for phase identification. TMA was performed using a Sucksmith balance. Finally, the microstructure and morphology of the powders and the particle grain size were studied by a Hitachi S-4000 FEG high-resolution scanning electron microscope (HRSEM).

3. Results and discussion

3.1. Process explanation

The magnetization curve for the initial powder synthesized conventionally is shown in Fig. 1. Note the steep initial magnetization behavior and an appreciable intrinsic coercivity (H_{ci}) of 315 kA/m. After nitrogenation at 950 °C for 5 h, under an initial gas pressure of 1 bar, the magnetic properties changed significantly. Fig. 2 shows there to be a significant decrease in the intrinsic coercivity from 315 to 179 kA/m but little change in M_m. There was a small decrease in the remanence from 38.1 J/Tkg to 30.8 J/Tkg.

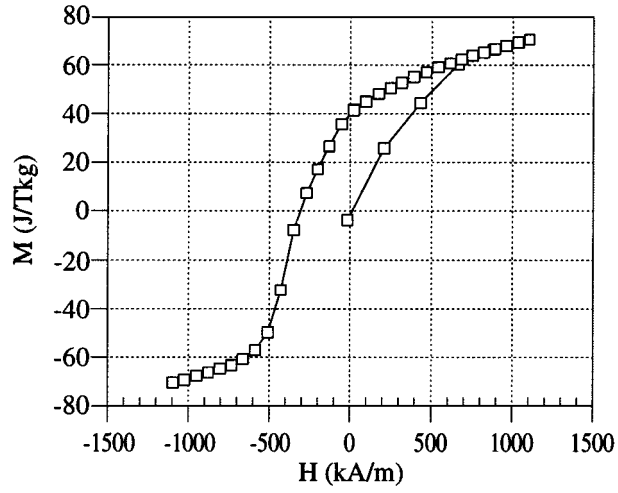

Figure 1 Magnetization curve for the conventionally synthesized starting powder.

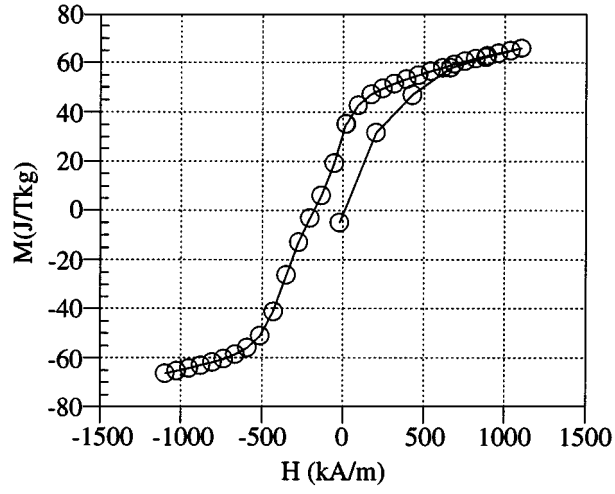

Figure 2 Magnetization curve for the initial powder, nitrogenated under 1 bar initial pressure at 950 °C for 5 h, showing an appreciable decrease in the intrinsic coercivity.

When this powder was re-calcined at 1000 °C for 1 h in air, the remanence (M_r) and M_m attained values very close to those of the initial powder, whereas the intrinsic coercivity attained a value of 340 kA/m, i.e., significantly higher than the initial value. There was also a significant decrease in the slope of the initial magnetization curve (see Fig. 3).

The comparative magnetic properties at each stage are indicated in Table 1. The XRD traces for the initial-, nitrogenated-, and re-calcined powders are shown in Fig. 4a, b, and c, respectively. All the peaks in Fig. 4a belong to the stoichiometric M-type strontium hexaferrite, $SrFe_{12}O_{19}$ or $SrO{\cdot}6Fe_2O_3$ [7].

The XRD traces in Fig. 4b reveal that some phase transformations had occurred during nitrogenation. Although the main phase is still strontium hexaferrite, there are now some other peaks that belong to Fe_3O_4

TABLE I Magnetic properties of the powder in the initial, nitrogenated, and re-calcined conditions

Sample	M_r (±3%, J/Tkg)	H_{ci} (±2%, kA/m)	M_m (±3%, J/Tkg)
Initial	38.1	314.6	67.55
Nitrogenated	30.8	179.3	66.43
Nitrogenated and Re-calcined	36.8	340.1	66.33

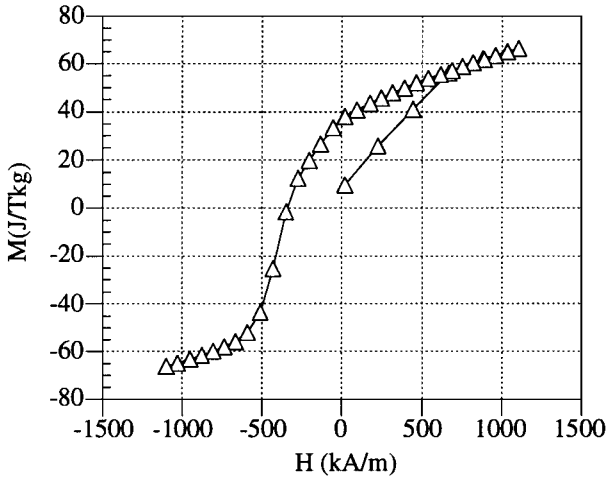

Figure 3 Magnetization curve for the nitrogenated powder calcined at 1000 °C for 1 h in air, showing an improved intrinsic coercivity.

and $Sr_7Fe_{10}O_{22}$ ($7SrO{\cdot}5Fe_2O_3$) [8, 9]. This indicates that the hexaferrite phase had decomposed partially into $Sr_7Fe_{10}O_{22}$ and Fe_2O_3, and then the Fe_2O_3 was reduced partially to Fe_3O_4. The decrease in the magnetic properties during this step, particularly the intrinsic coercivity, (Fig. 2) can thus be attributed to the presence of the magnetically soft Fe_3O_4 ($H_{ci} = 4$ A/m) phase [10]. The reduction of iron oxide did not proceed to the formation of FeO and Fe, stopping with magnetite (Fe_3O_4) formation [11, 12]. In addition to the major and minor phases indicated in Fig. 4b, a number of low-intensity peaks attributed to phases such as Fe_2O_3 (hematite), $SrFe_2O_5$, and Fe_3N [13–15] were also present.

In Fig. 4c, only the peaks due to the strontium–hexaferrite could be observed (similar to Fig. 4a). This indicates that, during re-calcination, the reduction products were again oxidized, leading to a recovery of the hexaferrite phase. The fact that the values obtained for the M_r and M_m in the initial and final powders were similar (Table I) confirms this finding and reveals that the reduction reactions occurring during nitrogenation are completely reversible.

The microstructures of the initial, nitrogenated, and re-calcined powders are presented in Figs 5, 6, and 7, respectively. Fig. 5 shows that the initial hexaferrite grains of the initial powder have smooth surfaces and sharp edges, i.e., a faceted morphology. Fig. 6 shows the detailed morphology of the hexagonal grains after nitrogenation. It can be seen that the formerly smooth edges of the grains have become chamfered, while some of the large single-crystal particles have been converted into particles with fine sub-grains. i.e., polycrystalline particles. This re-crystallization phenomenon appears

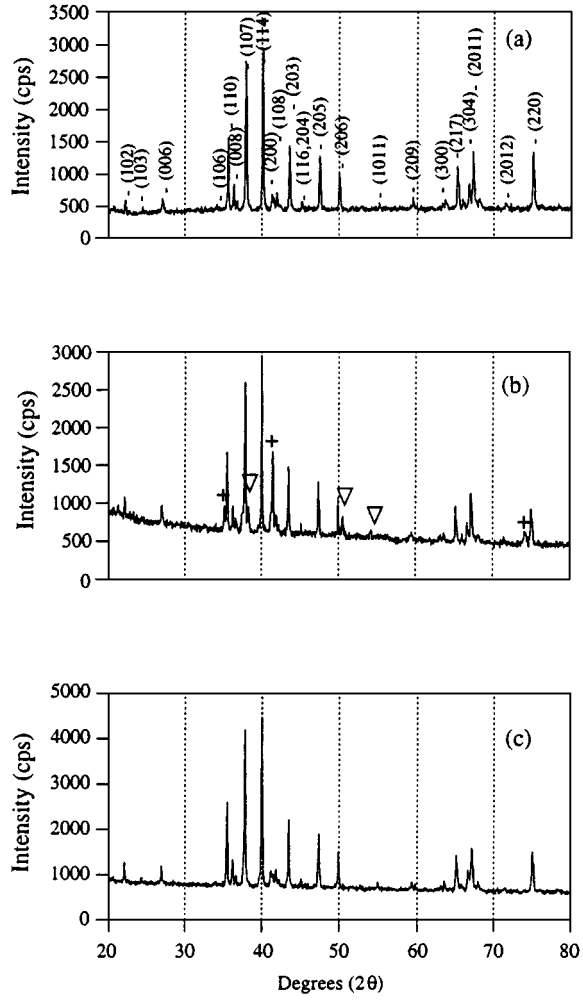

Figure 4 XRD traces of the powder in the (a) initial state; (b) after nitrogenation at 950 °C for 5 h under an initial pressure of 1 bar; and (c) after re-calcination at 1000 °C for 1 h in air. (+ = Fe_3O_4, ∇ = $Sr_7Fe_{10}O_{22}$).

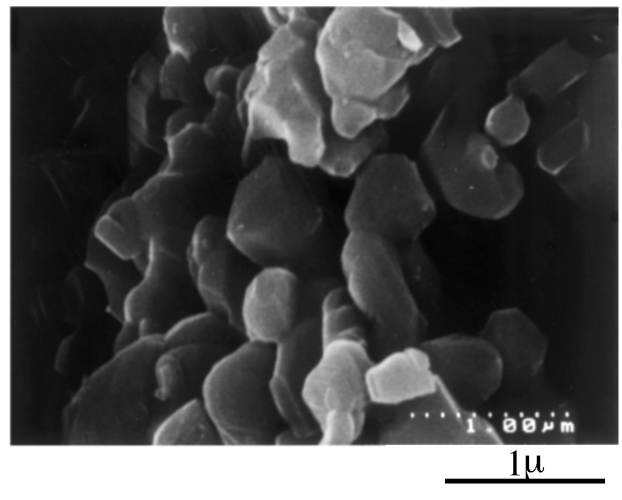

Figure 5 HRSEM micrograph of the initial single-crystal powder with smooth surfaces, sharp edges, and mean grain size below 500 nm.

to have a great influence on the size of the re-formed hexaferrite grains formed during re-calcination. Fig. 7 shows the fine grains that result. The mean grain size in the initial state (Fig. 5) was below 500 nm, whereas the mean grain size in the final state was much less.

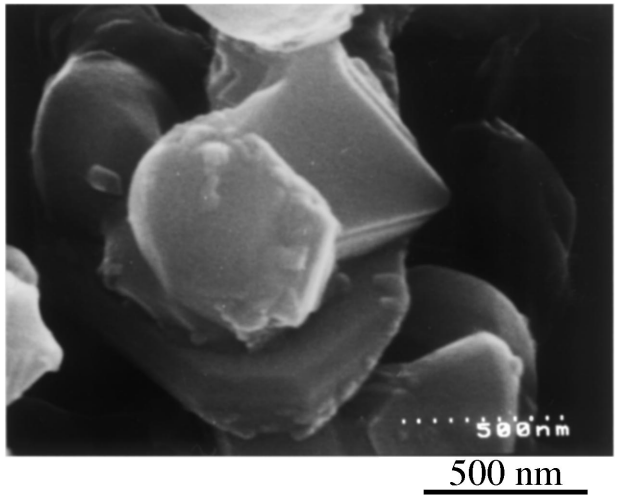

Figure 6 HRSEM micrograph of the hexaferrite powder after nitrogenation at 950 °C for 5 h under 1 bar initial pressure, showing the uneven grain edges.

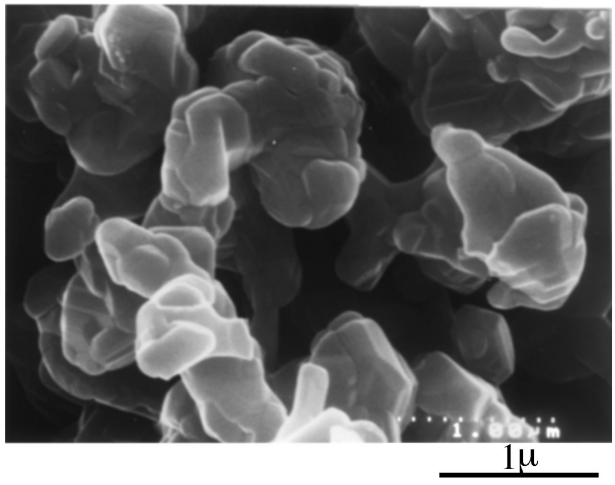

Figure 7 HRSEM micrograph of the conventionally synthesized strontium hexaferrite powder nitrogenated at 950 °C for 5 h under an initial pressure of 1.3 bar and re-calcined at 1000 °C for 1 h, showing polycrystalline particles with much finer grains than those of the initial powder.

The increase in the intrinsic coercivity on re-calcination (Fig. 3) in comparison with that of the initial powder (Fig. 1) can be attributed to this finer grain structure. The finer grain size is also consistent with the decrease in slope of the initial magnetization curve, which can be attributed to the single-domain behavior of some of the grains.

3.2. Process optimization

3.2.1. Nitrogenation temperature

The magnetic properties of conventionally synthesized strontium hexaferrite, nitrogenated under an initial pressure of 1 bar for 5 h at different temperatures and then calcined at 1000 °C for 1 h in air are shown in Fig. 8. Note that the maximum magnetization and the remanence show very little variation and can be considered as remaining essentially constant.

By contrast, the H_{ci} increased gradually from 227.3 kA/m after heat treatment at 600 °C to a maximum of 340.1 kA/m after heat treatment at 950 °C

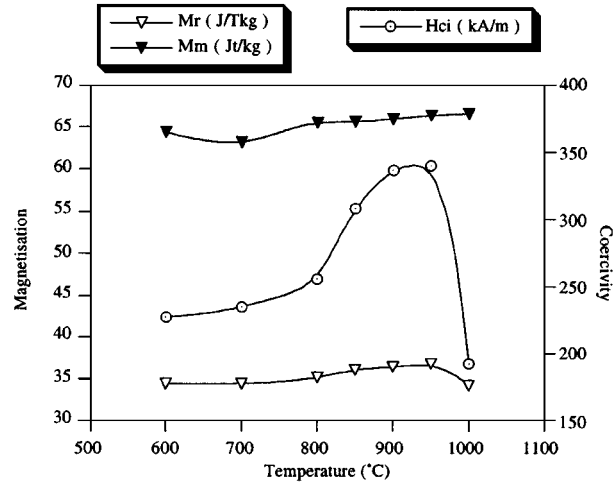

Figure 8 Magnetic properties of conventionally synthesized strontium hexaferrite powders nitrogenated for 5 h under an initial pressure of 1 bar at different temperatures and then re-calcined at 1000 °C for 1 h in air. (Typical error: remanence ±3%, coercivity ±2%).

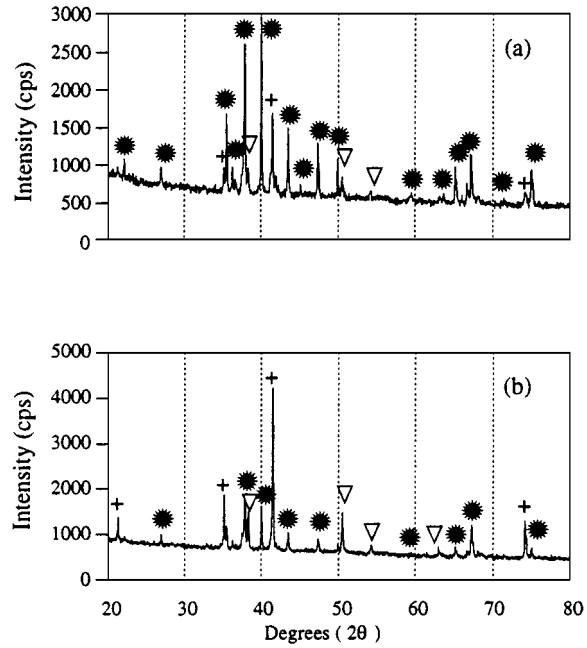

Figure 9 XRD traces for the conventionally synthesized strontium hexaferrite powder nitrogenated under 1 bar initial pressure for 5 h at (a) 950 °C (b) 1000 °C (✹ = Sr–hexaferrite, + = Fe_3O_4, ∇ = $Sr_7Fe_{10}O_{22}$).

and then decreased markedly at higher temperatures. The increase can be attributed to a progressively finer structure during re-calcination as a consequence of the fine grains produced during nitrogenation. Thus, as the nitrogenation temperature increased, the reduction process proceeded further (Fig. 9) with the formation of even finer grains. The marked decrease in coercivity at temperatures above 900 °C can therefore be correlated to significant grain growth.

Fig. 9a and b show the XRD traces of the Sr–hexaferrite powder nitrogenated for 5 h at 950 and 1000 °C, respectively. It can be seen that, at a nitrogenation temperature of 1000 °C, the reduction process was more advanced, with the Fe_3O_4 phase replacing the hexaferrite phase as the predominant phase. However, the growth

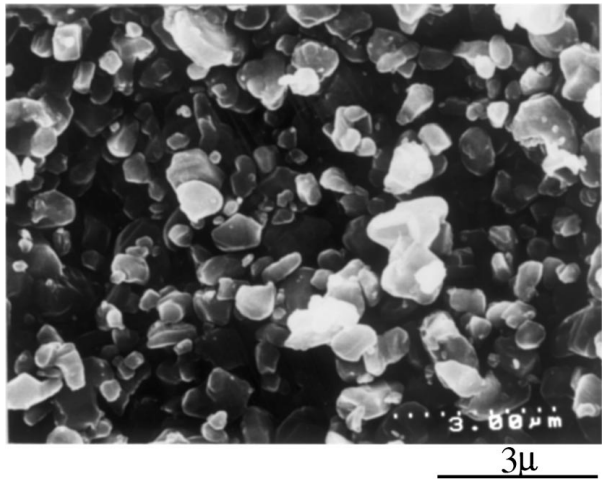

Figure 10 HRSEM micrograph of the conventionally synthesized strontium hexaferrite powder nitrogenated at 950 °C under an initial pressure of 1 bar for 5 h.

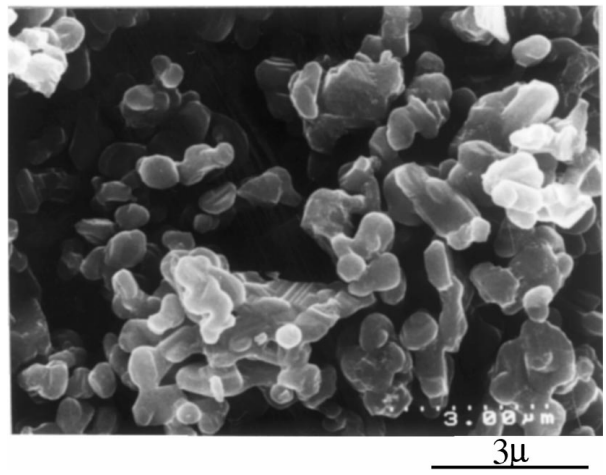

Figure 11 HRSEM micrograph of the conventionally synthesized strontium hexaferrite powder nitrogenated at 1000 °C under an initial pressure of 1 bar for 5 h. There is clear evidence of partial sintering of the particles.

of the grains also influenced the properties, so that beyond 950 °C the magnetic properties, notably coercivity, were more affected by the grain growth than by the progress in the reduction process and the formation of new fine grains. This resulted in a decrease in the intrinsic coercivity after recalcination. This change in grain size can be seen by comparing the microstructure of powders nitrogenated at 950 and 1000 °C, as shown in Figs 10 and 11, respectively. The powder in Fig. 10 has a much finer structure than that shown in Fig. 11.

Thus, the optimum temperature for nitrogenation is 950 °C under an initial pressure of 1 bar for 5 h, during which time the sample was not reduced fully, as shown in Fig. 9a.

3.2.2. Nitrogenation time

The results of the magnetic measurements for the strontium hexaferrite, synthesized conventionally and nitrogenated at 950 °C under an initial pressure of 1 bar for different times and then calcined at 1000 °C for 1 h in air, are shown in Fig. 12.

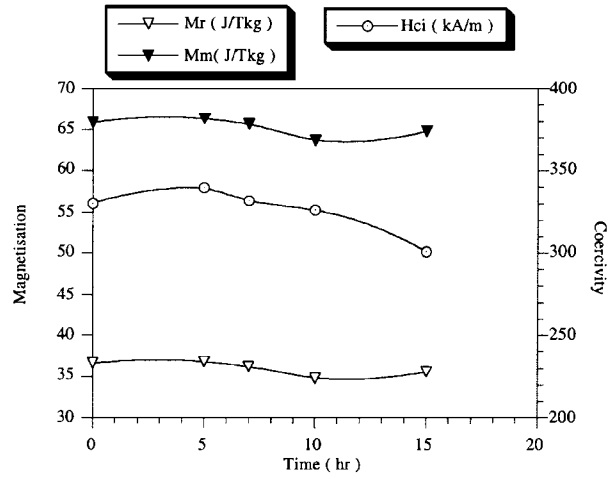

Figure 12 Magnetic properties of the conventionally synthesized strontium hexaferrite powder nitrogenated at 950 °C under 1 bar initial pressure for different times and then calcined at 1000 °C for 1 h in air. (Typical error: remanence ±3%, coercivity ±2%).

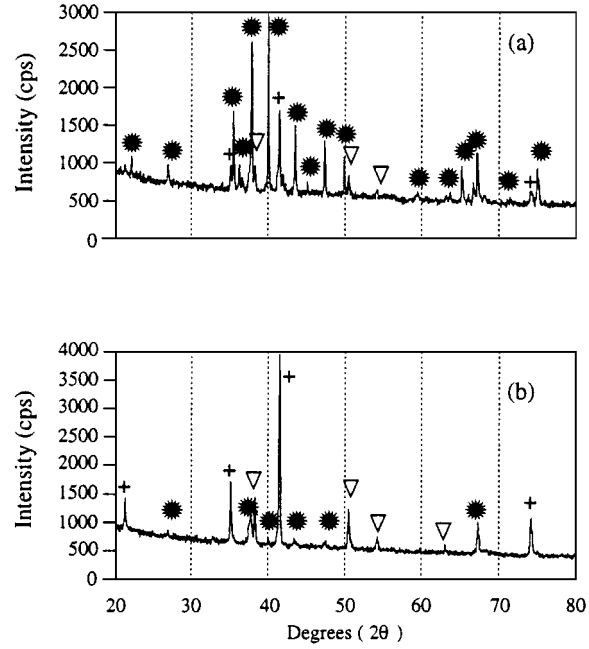

Figure 13 XRD traces for the conventionally synthesized Sr–hexaferrite powder nitrogenated at 950 °C under 1 bar initial pressure for (a) 5 h and (b) 15 h (✹ = Sr–hexaferrite, + = Fe_3O_4, ∇ = $Sr_7Fe_{10}O_{22}$).

The M_m and the remanence M_r were almost constant, fluctuating slightly above values of around 65 J/Tkg and 36 J/Tkg, respectively. The H_{ci}, on the other hand, increased to a maximum of 340.1 kA/m with increasing nitrogenation time (up to 5 h) and then gradually decreased with further increases in time. After nitrogenation times longer than 10 h, the decrease in the H_{ci} values was more marked.

Fig. 13a and b show the XRD traces for the Sr–hexaferrite powder nitrogenated at 950 °C under an initial pressure of 1 bar for 5 and 15 h, respectively. In Fig. 13a, the hexaferrite is the main phase but Fe_3O_4 and $Sr_7Fe_{10}O_{22}$ are also observed. In Fig. 13b, the main phase is now Fe_3O_4 with the hexaferrite being a minority phase. Thus, the reduction process proceeds further during a longer nitrogenation treatment.

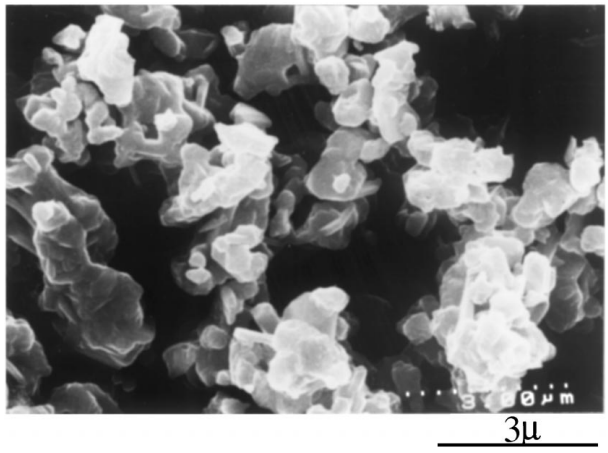

Figure 14 HRSEM micrograph of the conventionally synthesized strontium hexaferrite powder nitrogenated at 950 °C under an initial pressure of 1 bar for 15 h, showing the agglomeration and coarsening of the grains.

A comparison between the appearance of the powder nitrogenated at 950 °C for 5 h (Fig. 10) with that nitrogenated for 15 h (Fig. 14) shows the coarser structure of the latter powder, probably due to the agglomeration/coarsening of fine grains. This also resulted in a coarser structure after re-calcination.

Thus, the increase in the intrinsic coercivity with increasing nitrogenation time up to 5 h, as shown in Fig. 12, can be attributed to the finer grains re-forming as the hexaferrite during re-calcination, while the decrease after longer nitrogenation times can be ascribed to the coarser structure carried through to the re-calcination stage. Therefore, nitrogenation for 5 h (at 950 °C under 1 bar initial pressure) is the optimum treatment.

3.2.3. Initial nitrogenation pressure

The results of the magnetic measurements on the powders nitrogenated at 950 °C for 5 h under different initial pressures and then calcined at 1000 °C for 1 h in air are presented in Fig. 15.

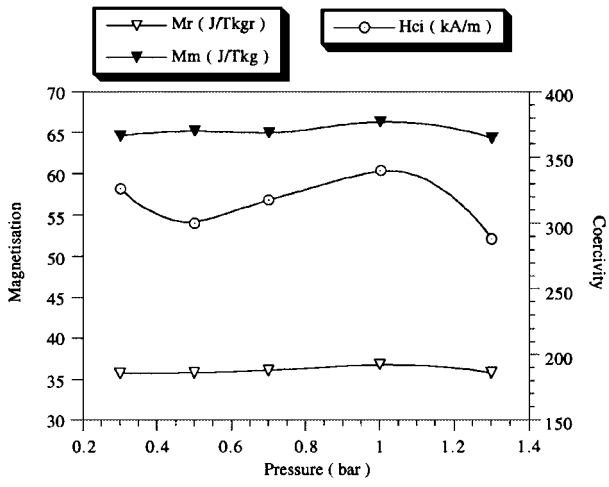

Figure 15 Magnetic properties of the conventionally synthesized strontium hexaferrite powder nitrogenated at 950 °C for 5 h under different initial pressures and then calcined at 1000 °C for 1 h in air. (Typical error: remanence ±3%, coercivity ±2%).

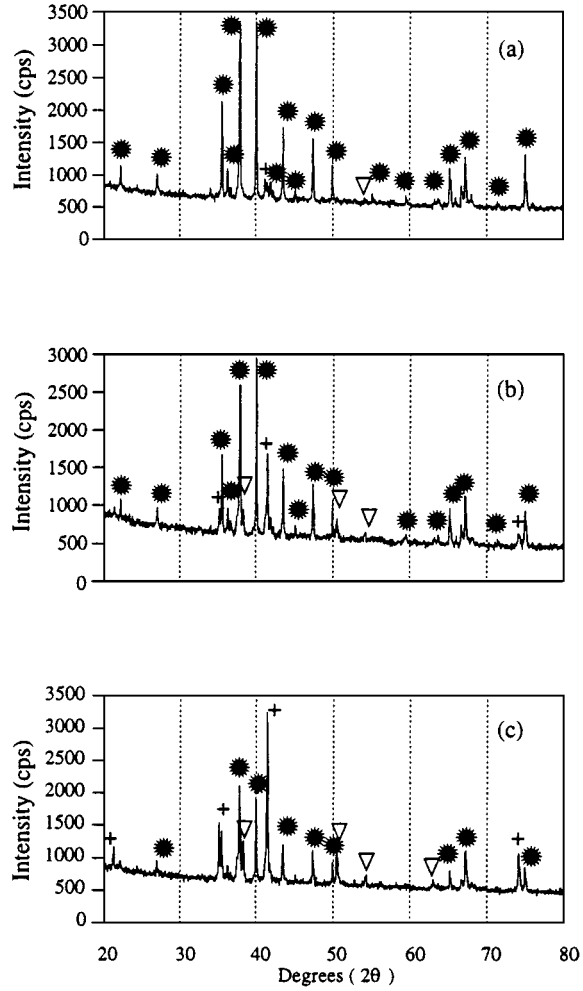

Figure 16 XRD traces for the conventionally synthesized strontium hexaferrite powder nitrogenated at 950 °C for 5 h under initial pressure of (a) 0.3 bar; (b) 1 bar; and (c) 1.3 bar (✹ = Sr–hexaferrite, + = Fe_3O_4, ∇ = $Sr_7Fe_{10}O_{22}$).

It can be seen that the M_m and the M_r fluctuated around 36 and 65 J/Tkg, respectively. The H_{ci}, after decreasing slightly at 0.5 bar, increased gradually with increasing initial nitrogen gas nitrogenation up to 1 bar (340.1 kA/m) and then dropped at higher initial pressures.

Fig. 16 shows the XRD traces of the powder nitrogenated at 950 °C for 5 h under initial pressure of 0.3, 1, and 1.3 bar, respectively.

In Fig. 16a, the powder is seen to consist almost entirely of the hexaferrite phase. In Fig. 16b, however the Fe_3O_4 and $Sr_7Fe_{10}O_{22}$ phases are now present together with the main hexaferrite phase. At 1.3 bar, shown in Fig. 16c, Fe_3O_4 has become the main phase with the peaks for the hexaferrite phase now being weaker. Thus, increasing the initial pressure, increased the degree of reduction and hence the proportion of fine sub-grains, and consequently the coercivity. However, comparing the structure of the powder nitrogenated at 950 °C for 5 h under an initial pressure of 1 bar (Fig. 10) with that of the powder nitrogenated at 950 °C for 5 h under an initial pressure of 1.3 bar (Fig. 17), it can be seen that there is more partial sintering and neck growth in the latter that resulted in a coarser structure after re-calcination. This would explain the decrease in

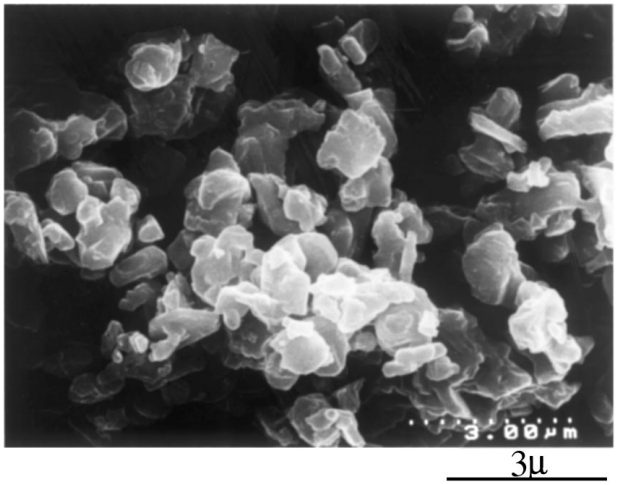

Figure 17 HRSEM micrograph of the conventionally synthesized strontium hexaferrite powder nitrogenated at 950 °C for 5 h under the initial pressure of 1.3 bar, showing the sub-division of big grains into fine sub-grains and agglomeration of the particles.

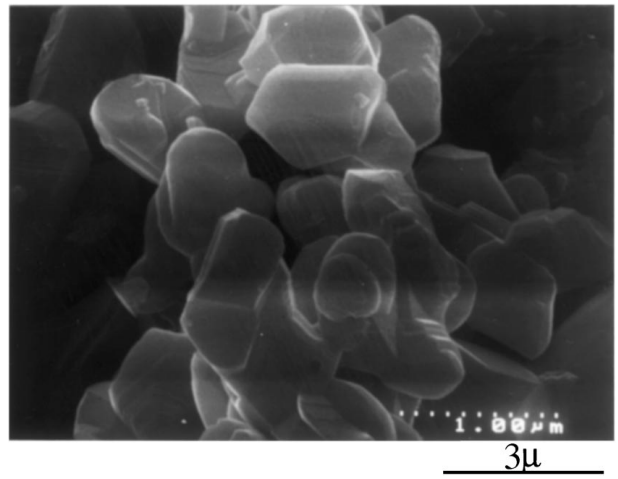

Figure 19 HRSEM micrograph of the conventionally synthesized strontium hexaferrite powder nitrogenated at 950 °C for 5 h under the initial pressure of 1.3 bar and re-calcined at 1100 °C for 1 h. This shows the coarsening of the grains.

the coercivity as the initial gas pressure was increased above 1 bar (see Fig. 15).

Under low initial gas pressures, below 0.5 bar (see Fig. 16a), the formation of phases other than the present hexaferrite phase was negligible. Thus, the re-calcination of the samples after nitrogenation at these pressures is essentially just the re-calcination of the initial powder, which results in grain growth and hence a decrease in the coercivity. This would explain the slight decrease in the coercivity of the sample re-calcined after nitrogenation under 0.5 bar initial pressure (see Fig. 15). Therefore, the optimum initial nitrogenation pressure seems to be around 1 bar.

3.2.4. Re-calcination temperature

The magnetic properties of the conventionally synthesized hexaferrite powder nitrogenated optimally at 950 °C for 5 h under an initial gas pressure of 1 bar and then calcined at different temperatures for 1 h in air are shown in Fig. 18.

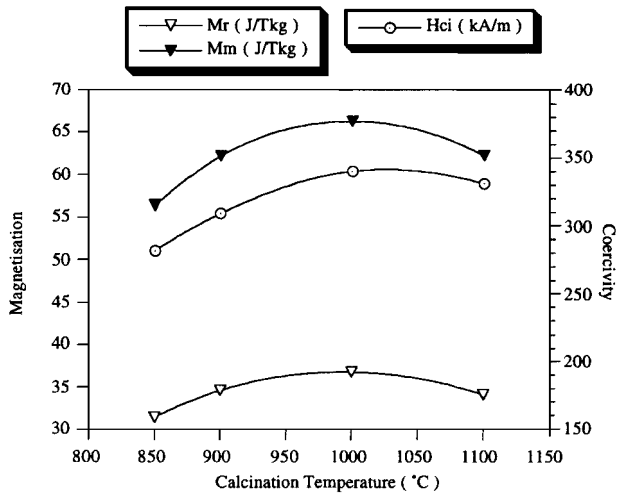

Figure 18 Magnetic properties of the conventionally synthesized strontium hexaferrite powder nitrogenated at 950 °C for 5 h under the initial pressure of 1 bar and then calcined at different temperatures for 1 h in air. (Typical error: remanence ±3%, coercivity ±2%).

All the magnetic properties increase with increasing re-calcination temperature up to 1000 °C and then decrease slightly. The decrease in the coercivity at re-calcination temperatures above 1000 °C can be attributed to grain growth. This can be seen by comparing the microstructure of the nitrogenated powder, re-calcined at 1000 °C (Fig. 7) with that of the nitrogenated powder re-calcined at 1100 °C (Fig. 19). The latter shows evidence of grain growth. The decrease in the remanence and saturation magnetization values at re-calcination temperatures above 1000 °C might be related to the partial decomposition of the ferrite phase. Thus, it can be deduced that the re-formation of hexaferrite phase was completed at 1000 °C and this temperature is the optimum re-calcination temperature.

4. Conclusions

During the nitrogenation process, the strontium hexaferrite decomposes and the resultant iron oxide (Fe_2O_3) is reduced, causing the hexaferrite particles/grains to be divided into very fine sub-grains. The extent of this process depends on the conditions but even at the higher degrees of nitrogenation, the reduction of Fe_2O_3 only resulted in the formation of Fe_3O_4 with no traces of FeO or Fe being observed. In addition to Fe_3O_4, $Sr_7Fe_{10}O_{22}$ was the other main phase formed as a result of nitrogenation. The main effect of the process on the magnetic properties was a significant decrease in the intrinsic coercivity because of the magnetically softer nature of Fe_3O_4. With a subsequent calcination process, the reactions were reversed and the hexaferrite phase re-formed. As a result of this, the maximum magnetization and the remanence showed values very close to the initial values, but the intrinsic coercivity exhibited a significantly higher value due to the much smaller grain size, which originated from the fine sub-grain structure formed during nitrogenation. The finer grain size also influenced the initial magnetization curve that exhibited a diminished slope compared to that of the original material. The optimized conditions were static nitrogenation at 950 °C for 5 h under 1 bar initial gas

pressure followed by calcination in static air at 1000 °C for 1 h. The highest value obtained for the intrinsic coercivity was ∼ 340 kA/m.

Acknowledgements

Thanks are due to the members of the Applied Alloy Chemistry Group (School of Metallurgy and Materials) for their co-operation. The financial support of Tehran University is gratefully acknowledged.

References

1. A. ATAIE, I. R. HARRIS and C. B. PONTON, Patent Application No. PCT/GB95/02758, November 1995.
2. A. ATAIE, C. B. PONTON and I. R. HARRIS, *J. Mat. Sci.* **20** (1996) 5521–5527.
3. S. A. EBRAHIMI, A. J. WILLIAMS, N. MARTINEZ, A. ATAIE, A. KIANVASH, C. B. PONTON and I. R. HARRIS, *J. Phys. IV* **7** (1997) C1 325.
4. S. A. EBRAHIMI, A. KIANVASH, C. B. PONTON and I. R. HARRIS, *J. Mat. Sci.* **34** (1999) 35–43.
5. N. MARTINEZ, S. A. EBRAHIMI, A. J. WILLIAMS and I. R. HARRIS, *J. Mat. Sci.* (1999) in press.
6. S. A. EBRAHIMI, A. KIANVASH, C. B. PONTON and I. R. HARRIS, *J. Mat. Sci.* **34** (1999) 53–58.
7. V. ADELSKOLD, *Arkive for Kemi, Min. Geol.* **12A** (1938) 1; JCPDS/24-1207.
8. National Bureau of Stand, Monograph 25, 5 31, 1967; JCPDS/19-629.
9. E. LUCCHINI, D. MINICHELLI and G. SLOCCARI, *J. Am. Ceram. Soc.* **57** (1974) 42; JCPDS/26-980.
10. G. BATE, in "Magnetic Oxides," edited by D. J. Craik (John Wiley & Sons, 1975) Part 2, Chapter 12, pp. 689–742.
11. T. YAGI, T. SUZUKI and A. AKIMOTO, *J. Geophys. Res.* **90** (1985) 8784; JCPDS/39-1088.
12. H. E. SWANSON, NBS Circular 539, **4** (1955) 3; JCPDS/6-0696.
13. National Bureau of Standards, Monograph 25, 18 37, 1981; JCPDS/33-664.
14. S. SHIN, *Mater. Res. Bull.* **13** (1978) 1017; JCPDS/33-677.
15. J. HANAWALT, H. RINN and L. FREVEL, *Anal. Chem.* **10** (1938) 457; JCPDS/1-1236.

Received 19 June
and accepted 6 August 1998